Synthesis, characterization and luminescence properties of homoleptic platinum(II) acetylide complexes †

José Benito,[a] Jesús R. Berenguer,[a] Juan Forniés,*[b] Belén Gil,[a] Julio Gómez[a] and Elena Lalinde *[a]

[a] *Departamento de Química-Grupo de Síntesis Química de La Rioja, UA-CSIC, Universidad de La Rioja, 26006, Logroño, Spain. E-mail: elena.lalinde@dq.unirioja.es*

[b] *Departamento de Química Inorgánica, Instituto de Ciencia de Materiales de Aragón, Universidad de Zaragoza-Consejo Superior de Investigaciones Científicas, 50009 Zaragoza, Spain. E-mail: forniesj@posta.unizar.es*

A family of homoleptic tetraalkynylplatinate(II) complexes $(NBu_4)_2[Pt(C{\equiv}CR)_4]$ containing various arylsubstituted $(R = C_6H_4X)$, where X is an electron-donating, -withdrawing or -delocalizing substituent, and ethynylpyridine (C_5H_4N-2, C_5H_4N-4) ligands have been prepared. The structures of complexes with $R = (4\text{-}CF_3)C_6H_4$ ($\mathbf{4}{\cdot}2HCCl_3$), $(4\text{-}CN)C_6H_4$ ($\mathbf{6}{\cdot}H_2O$) and C_5H_4N-4 ($\mathbf{9b}{\cdot}HC{\equiv}CC_5H_4N-4{\cdot}2H_2O$) have been determined by single-crystal X-ray diffraction. While in the case of $\mathbf{4}$ two molecules of $CHCl_3$ are incorporated to the anion by short $CH \cdots \pi$ interactions, for the *para*-pyridylethynyl derivative one H_2O molecule connect different anions through moderate $N \cdots H–O–H \cdots N$ intermolecular interactions, giving an extended one-dimensional chain. The photophysical and electrochemical properties of the complexes have been examined. All of them display emissions at 77 and 298 K in the fluid and solid state, with lifetimes in the microsecond regime. In some cases the emission profile is clearly the envelope of several closely bands, whose relative intensity depends on the excitation energy. On the basis of TD-DFT theoretical calculations on the anion $[Pt\{C{\equiv}C(4\text{-}CN)C_6H_4\}_4]^{2-}$ of complex $\mathbf{6}$, it is proposed that the emissions are due to triplet intraligand excited states, with both an aryl (or pyridyl) and acetylenic character, which arise from an admixture of $\pi \longrightarrow \pi^*(C{\equiv}CR)$ IL and $d_\pi(Pt) \longrightarrow \pi^*(C{\equiv}CR)$ MLCT transitions.

Introduction

Interest in the synthesis and characterization of platinum alkynyl-containing complexes[1–5] has grown rapidly in recent years, particularly due to their widespread potential application in material science. Tremendous efforts have been devoted to the preparation of rigid-rod olygomers and polymers, not only of platinum, but also of nickel and palladium, because of their remarkable electronic and optoelectronic properties.[6–11] Recently, a number of interesting hyperbranched or dendritic molecules of platinum, containing alkynyl ligands as the organic backbone,[12–15] and also macrocycles,[16–20] have been reported. On the other hand, diimine or polypyridyl alkynyl platinum species have also been extensively explored, due to their intriguing spectroscopic and luminescence properties owing to the presence of π–π stacking and/or metal–metal interactions.[15,21–26] In this field, increasing attention has currently been paid to the study of the spectroscopic and luminescence behaviour of discrete polynuclear platinum complexes containing alkynyl bridging ligands, because they offer interesting possibilities of modulation by metal $\cdots$ metal and η^2-metal alkynyl bonding interactions.[27–30] Within this framework, we have previously shown that the homoleptic $(NBu_4)_2[Pt(C{\equiv}CR)_4]$ ($R = Ph$, ^tBu, $SiMe_3$) are excellent precursors for the preparation of clusters or heteropolynuclear $Pt–Cu$,[31,32] $Pt–Ag$,[33,34] $Pt–Tl$[35–37] or $Pt–Cd$,[38,39] which exhibit luminescence properties that are associated with $Pt \cdots Pt$, $Pt \cdots M$ and $\eta^2 \cdots M$ alkynyl bonding interactions.

In an attempt to obtain further insights into the role played by the alkynyl ligands, as well as their relation to the extent of metal-metal interactions, in the spectroscopic and excited-state properties of the final heteropolynuclear platinum clusters, we focused our interest on new homoleptic anionic platinum substrates with different alkynyl groups. Although σ-bonded neutral and cationic alkynyl platinum complexes have been thoroughly investigated, the number of reports on mononuclear anionic derivatives[40–50] is very small and, as far as we know, only the crystal structure of $(NBu_4)_2[Pt(OBET)_2]$ (OBET = dianion of 2,2′-diethynyltolane) has been reported.[50]

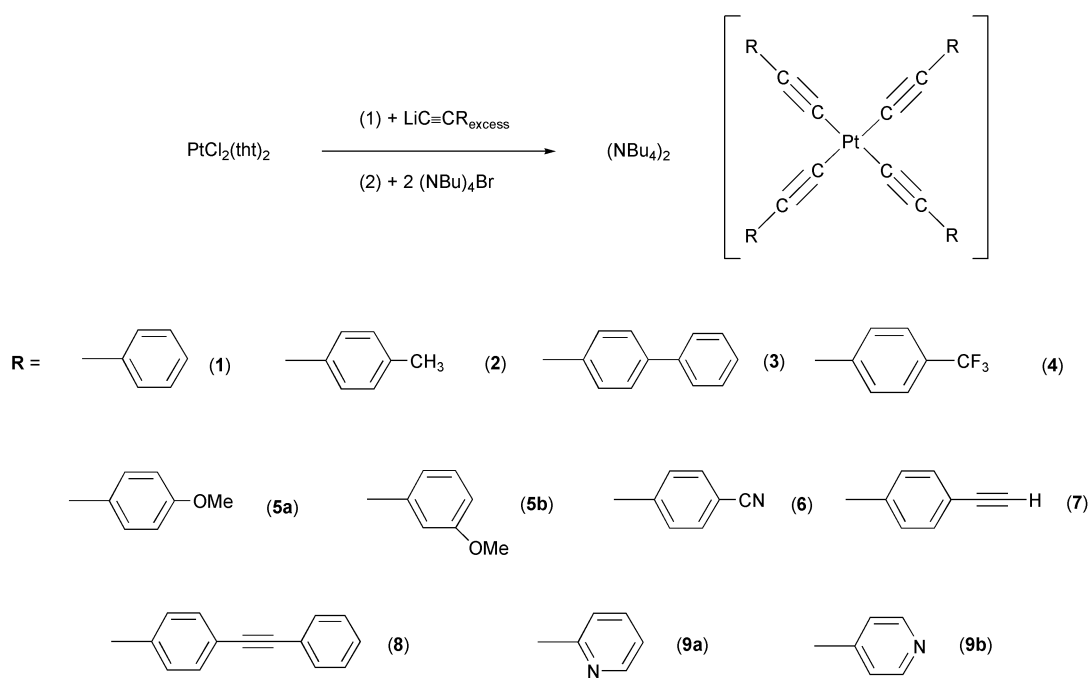In this paper, we report the synthesis and characterization of a novel series of homoleptic derivatives $(NBu_4)_2[Pt(C{\equiv}CR)_4]$ ($\mathbf{1}$–$\mathbf{9}$), together with the structural characterization of $(NBu_4)_2[Pt\{C{\equiv}C(4\text{-}CF_3)C_6H_4\}_4]{\cdot}2HCCl_3$ ($\mathbf{4}{\cdot}2HCCl_3$), $(NBu_4)_2[Pt\{C{\equiv}C(4\text{-}CN)C_6H_4\}_4]{\cdot}H_2O$ ($\mathbf{6}{\cdot}H_2O$) and $(NBu_4)_2[Pt(C{\equiv}CC_5H_4N-4)_4]{\cdot}HC{\equiv}CC_5H_4N-4{\cdot}2H_2O$ ($\mathbf{9b}{\cdot}HC{\equiv}CC_5H_4N-4{\cdot}2H_2O$). We also examine their photophysical and electrochemical properties.

Results and discussion

Synthesis and spectroscopic properties

A series of tetraalkynyl platinate $(NBu_4)_2[Pt(C{\equiv}CR)_4]$ complexes $\mathbf{1}$–$\mathbf{9}$ (Scheme 1) was synthesized, characterized and its photophysical properties studied. The synthesis has been carried out following a similar procedure to that of complexes $(NBu_4)_2[Pt(C{\equiv}CR)_4]$ ($R = Ph$, ^tBu, $SiMe_3$), described elsewhere by us,[45,48] or $(NBu_4)_2[Pt(OBET)_4]$, reported by Tessier and Youngs.[50] $Li_2[Pt(C{\equiv}CR)_4]$ was readily formed by the reaction of the platinum dichloride complex $[PtCl_2(tht)_2]$ (tht = tetrahydrothiophene) with an excess of $LiC{\equiv}CR$ (5.5–8.5 equiv. generated *in situ* from ^nBuLi and the corresponding $RC{\equiv}CH$) in 50 cm³ of Et_2O or THF ($\mathbf{9b}$). The tetrabutylammonium salts $(NBu_4)_2[Pt(C{\equiv}CR)_4]$ were prepared, as white ($\mathbf{1}$), yellow ($\mathbf{2}$–$\mathbf{8}$, $\mathbf{9b}$) or pale-brown ($\mathbf{9a}$) solids, in low-moderate to high yield (22–90%) by removing the ether from the reaction mixture, dissolving $Li_2[Pt(C{\equiv}CR)_4]$ in cold deoxygenated water (~40 cm³) or iso-

Scheme 1

propyl alcohol (~20 cm³, for complexes **3** and **8**), filtering through Celite and treating the filtrate with NBu$_4$Br. Using this methodology complexes **5a**, **7** and **9b** crystallize with two molecules of H$_2$O. In the synthesis of complex **9a**, the oily final precipitate is dissolved in CH$_2$Cl$_2$, and the solution dried with anhydrous MgSO$_4$ and evaporated to dryness. The addition of cold diethyl ether gives **9a** as a brown solid.

All these new compounds (except **7**, which has only a limited stability) are stable in the solid state at low temperature (-30 °) for months, but decompose in solution in a few hours at room temperature. They were satisfactorily characterized by spectroscopic (IR, ^{1}H and ^{13}C RMN and MS) and analytical methods. Some spectroscopic data [$\tilde{v}_{max}$(C≡C), δC_α and δC_β] are listed in Table 1. Data of the analogous ^{t}Bu and SiMe$_3$ derivatives, are also included for comparison. The IR spectra display a characteristic $\tilde{v}_{max}$(C≡C) absorption band between 2073 and 2086 cm^{-1}. These values lie at the low end reported for terminal alkynyl ligands, suggesting that, in these anionic systems, the Pt atom is probably a good π-back donor towards the π^* orbital of the alkynyl ligands, which weakens the corresponding C≡C bonds. Complex **8** exhibits one additional band at higher frequency (2209 cm^{-1}) due to the outer C≡CPh fragments, while complex **7** only shows a sharp additional signal at 3200 cm^{-1} attributed to ≡C–H stretching of the terminal C≡C–H unit. The mass spectra of all complexes show peaks related to the molecular anion [Pt(C≡CR)$_4$]$^-$ [M]$^-$, with the exception of complexes **2** and **8**, for which the peaks corresponding to the anion [Pt(C≡CR)$_3$]$^-$ were found. Thus, the ES($-$) mass spectra of complexes **4**, **5b**, **6** and **9a** show the peaks of their respective molecular ion [M]$^-$ at the expected m/z values, as well as the corresponding ion pairing {[M](NBu$_4$)} for complexes **3**, **7** and **9b** or {[M](NBu$_4$)$_2$} for complex **5a**.

The resonances of the C$_\alpha$ and C$_\beta$ alkynyl carbons, which are easily identifiable due to the significantly different coupling constants to the ^{195}Pt nucleus (Table 1), are of particular interest in the ^{13}C{^{1}H} NMR spectra. In all cases, the resonance corresponding to the alkyne C$_\alpha$ carbon is found at higher frequencies than the C$_\beta$ atom (δC_α 115.8–125.0 $vs.$ δC_β 101.2–105.2). A similar feature is found in CDCl$_3$ for (NBu$_4$)$_2$-[Pt(C≡CSiMe$_3$)$_4$], but with a more notable difference [δC_α/C$_\beta$ 140.4/104.4],[51] and this can be attributed to the β-negative inductive effect of the SiMe$_3$ group (Pt–$^+$C=C–$^-$SiMe$_3$). In contrast to this, in the homoleptic derivative containing the

electron donor *tert*-butyl group (NBu$_4$)$_2$[Pt(C≡C^{t}Bu)$_4$], the C$_\alpha$ alkynyl resonance is notably shifted upfield, and it is seen (δC_α 98.9) at lower frequencies than C$_\beta$ (δ 108.4).[51] The observed platinum-carbon coupling constants [^1J(Pt–C$_\alpha$) 984.0–1003.0 Hz; ^2J(Pt–C$_\beta$) 286.0–290.2 Hz] are similar to those found in the ^{t}Bu and SiMe$_3$ derivatives, and are comparable to those previously found in some neutral complexes of type [*trans*-Pt-(C≡CR)$_2$L$_2$] ([*trans*-Pt(C≡CPh)$_2$(PPh$_2$H)$_2$] δC_α 102.9, ^1J(Pt–C) 834 Hz; δC_β 112.4, ^2J(Pt–C) 259 Hz).[52] As expected for complexes **7** and **8**, the acetylene carbons of the outer acetylenic fragments are found at relatively upfield chemical shifts ($\delta C^5/C^6$ 80.6/86.0 **7**; 94.0/95.4 **8**).

The molecular structures of complexes **4** and **9b** are shown in Figs. 1 and 2 (for complex **6**, see Fig. S1 in ESI †). Selected bond distances and angles are given in Table 2. For complexes **4** and **6**, crystals were obtained by slow diffusion of *n*-hexane into saturated solutions of the compounds in CHCl$_3$ (**4**) or acetone (**6**) at low temperature (-40 °C). In the case of complex **9b**, the resulting aqueous filtrate after the precipitation of **9b** as a solid (see Experimental section) was left to evaporate at room
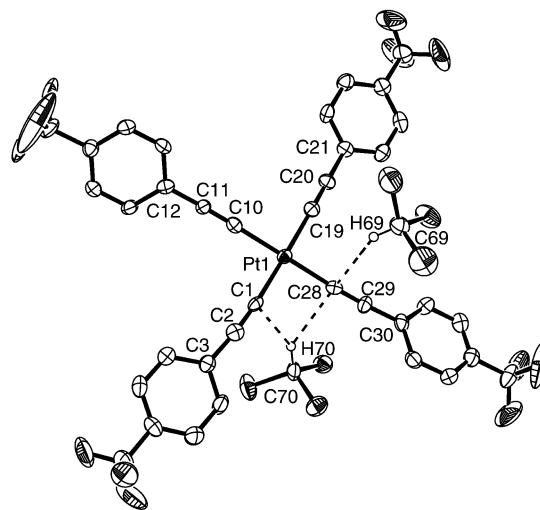

Fig. 1 ORTEP view of the anion [Pt{C≡C(4-CF$_3$)C$_6$H$_4$}$_4$]$^{2-}$ **4**, showing the interaction with the two molecules of CHCl$_3$. Ellipsoids are drawn at the 50% probability level. Hydrogen atoms have been omitted for clarity.

Table 1 δ_C of $C_\alpha\equiv C_\beta$ (^{13}C NMR recorded at -50 °C in CD_3COCD_3) and $\tilde{\nu}_{max}(C\equiv C)$ (in KBr pellets) of complexes **1–9**

Complex	R	δC_α ($^1J_{Pt-C}$/Hz)	δC_β ($^2J_{Pt-C}$/Hz)	$\tilde{\nu}_{max}(C\equiv C)$/cm^{-1}
1		120.9 (989.8)	104.1 (287.4)	2075 (s)
2	—⟨⟩—CH$_3$	118.4 (989.2)	102.1 (290.2)	2081 (s)
3[a]	—⟨⟩—⟨⟩	117.4 (984.0)	103.6 (285.0)	2082 (s)
4	—⟨⟩—CF$_3$	125.0 (997.0)	103.0 (286.3)	2084 (vs)
5a·2H$_2$O	—⟨⟩—OMe	115.8 (990.5)	101.2 (286.0)	2085 (vs)
5b	—⟨⟩—OMe	119.4 (990.2)	102.6 (288.1)	2078 (s)
6	—⟨⟩—CN	119.3[b]	104.1 (288.0)	2080 (vs), 2041 (sh)
7·2H$_2$O	—⟨⟩—≡—H	124.0 (993.0)	103.2 (289.0)	2073 (vs br) $\tilde{\nu}$(C–H) 3200 (s)
8	—⟨⟩—≡—⟨⟩	124.6 (1003.0)	104.0 (286.0)	2209 (m, C≡CPh) 2075 (s br, PtC≡C)
9a[c]		120.5 (991.7)	105.2 (287.0)	2081 (vs), 2059 (sh)
9b[a]		123.3 (995.7)	102.6 (297.7)	2086 (s), 2039 (sh)
(NBu$_4$)$_2$[Pt(C≡C^{t}Bu)$_4$]·2H$_2$O^{c,d}		98.9 (975.0)	108.4 (279.0)	2081 (m)
(NBu$_4$)$_2$[Pt(C≡CSiMe$_3$)$_4$]·2H$_2$O^{c,d}		140.4 (924.0)	104.4 (250.4)	2015 (s)

[a] ^{13}C NMR in CDCl$_3$ at -50 °C. [b] Tentatively assigned. [c] ^{13}C NMR in CDCl$_3$ at r.t.; [d] Ref. 51.

Table 2 Selected bond lengths (Å) and angles (°) for (NBu$_4$)$_2$[Pt{C≡C(4-CF$_3$)C$_6$H$_4$}$_4$]·2CHCl$_3$ (**4·2CHCl$_3$**), (NBu$_4$)$_2$[Pt{C≡C(4-CN)C$_6$H$_4$}$_4$]·H$_2$O (**6·H$_2$O**) and (NBu$_4$)$_2$[Pt(C≡CC$_5$H$_4$N-4)$_4$]·HC≡CC$_5$H$_4$N-4·2H$_2$O (**9b·HC≡CC$_5$H$_4$N-4·2H$_2$O**)

	4·2CHCl$_3$	**6**	**9b·HC≡CC$_5$H$_4$N-4·2H$_2$O**
Pt–C$_\alpha$	1.993(5), 2.005(5), 2.007(5), 2.007(5)	2.019(9), 1.992(10)	1.952(10), 1.966(10), 2.035(9), 2.047(10)
C$_\alpha$–C$_\beta$	1.215(7), 1.207(7), 1.208(7), 1.209(7)	1.170(11), 1.217(11)	1.146(13), 1.179(12), 1.238(12), 1.257(13)
cis-C$_\alpha$–Pt–C$_{\alpha'}$	92.2(2), 87.7(2), 91.0(2), 89.1(2)	91.7(3)	88.7(5), 89.45(18), 88.4(2), 93.5(4)
Pt–C$_\alpha$–C$_\beta$	175.7(8), 177.9(5), 176.6(6), 176.8(5)	177.4(9), 176.6(9)	172.4(9), 174.3(8), 173.2(8), 177.8(8)
C$_\alpha$–C$_\beta$–C$_{ipso}$	174.8(9), 178.4(6), 178.5(6), 176.7(6)	175.2(11), 176.9(11)	174.6(11), 175.4(10), 179.4(9), 176.4(9)
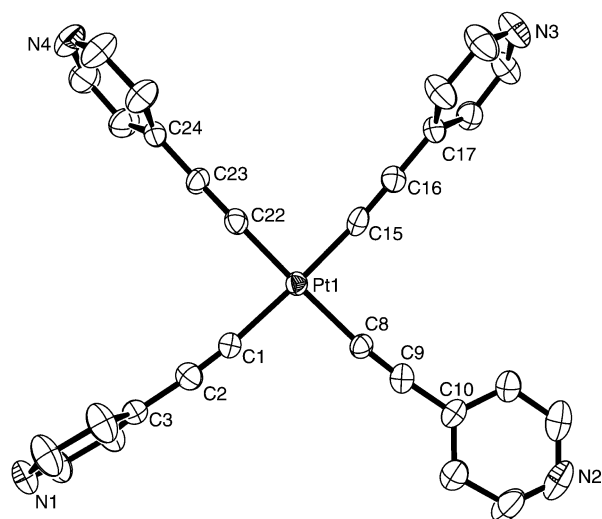
Fig. 2 View of the molecular structure of the anion [Pt(C≡CC$_5$H$_4$N-4)$_4$]$^{2-}$ **9b**. Ellipsoids are drawn at the 50% probability level. Hydrogen atoms have been omitted for clarity.

temperature overnight, yielding yellow crystals of **9b** crystallized with a molecule of *para*-ethynylpyridine and two molecules of water. To our surprise, in the case of the *para*-(trifluoromethyl)phenylethynyl derivative **4**, the complex crystallizes with two molecules of CHCl$_3$, which are incorporated to the anion through short C–H ··· π interactions. The presence of weak ≡C–H ··· π interactions in the crystal structures of organic alkynes seems to be a relatively common feature.[53] However, recent theoretical calculations by Lin and Mingos,[54] indicate that the donor potential of C≡C moieties bonded to metal atoms exceeds that found in purely organic alkynes. In particular, structural evidence for the existence of very robust C–H ··· π(alkyne) interactions has recently be shown in the crystal studies of the chloroform solvates [LAuC≡CAuL-(CHCl$_3$)$_2$] [L = PPh$_2$(naphthyl)] and [LAuC≡CAuL(CHCl$_3$)$_6$] [L = PPh(naphthyl)$_2$] with short Cl$_3$C–H ··· C(alkyne) distances ranging from 2.446 to 2.587 Å.[55–57] Weaker C(Cp)–H ··· C≡C contacts, with H ··· C distances in the range of 2.6 to 2.9 Å, have been also observed in cyclopentadienyl alkynyl complexes.[58] In the complex anion of **4** (Fig. 1), one of the chloroform molecules lies below the platinum coordination plane [H(70)CCl$_3$], and mainly interacts with both C$_\alpha$ carbon

Table 3 Absorption (~2×10^{-5} M solutions) and electrochemical data for complexes **1–9**

Compound	Absorption/nm ($10^3 \, \varepsilon$/M^{-1} cm^{-1})	E^{ox}/V
1	288 (40.4), 335 (33.8), 347 (30.3) (sh) (CH$_2$Cl$_2$)	0.608
	333 (43.4) (acetone)	
	286 (83.1), 336 (85.2) (sh), 346 (88.8) (toluene)	
	300 (50.5), 326 (39.8) (sh) (CH$_3$CN)	
2	285 (49.5), 334 (38.6), 345 (34.8) (sh) (CH$_2$Cl$_2$)	0.594
	335 (55.7) (acetone)	
	285 (63.2), 335 (63.0) (sh), 348 (76.3) (toluene)	
	286 (62.9), 334 (35.2) (sh) (CH$_3$CN)	
3	352 (52.1), 370 (49.3)[a] (CH$_2$Cl$_2$)	0.650
4	309 (48.5), 350 (44.7) (sh) (CH$_2$Cl$_2$)	0.804
	329 (62.6), 354 (52.0) (sh) (acetone)	
	310 (40.3), 352 (61.0), 365 (56.8) (sh) (toluene)	
	313 (80.1), 346 (51.3) (sh) (CH$_3$CN)	
5a	283 (62.0), 327 (46.4), 344 (53.0) (CH$_2$Cl$_2$)	0.516
5b	287 (49.7), 307 (40.7), 341 (50.0), 347 (49.0) (CH$_2$Cl$_2$)	0.720
6	338 (76.0), 368 (72.4), 381 (65.02) (sh) (CH$_2$Cl$_2$)	0.924
	351 (82.3), 389 (55.2) (sh) (acetone)	
	330 (40.3) (sh), 368 (56.1), 383 (48.7) (toluene)	
	294 (35.5) (sh), 338 (88.3), 364 (64.8) (sh) (CH$_3$CN)	
7	330 (81.9), 358 (82.3), 376 (80.0) (sh) (CH$_2$Cl$_2$)	0.730
8	283 (61.9), 374 (114.7)[b] (CH$_2$Cl$_2$)	0.666
9a	281 (24.7), 316 (25.5), 335 (23.5) (sh), 400 (5.0) (CH$_2$Cl$_2$)	0.916
9b	345 (48.4), 398 (34.0) (CH$_2$Cl$_2$)	0.844

[a] Very broad, with a long tail extending to *ca*. 410 nm. [b] Very broad, with a long tail extending to *ca*. 440 nm.

atoms of two mutually *cis* alkynyl groups [H(70) ··· C(1), C(28) 2.572, 2.594 Å]. The second molecule of HCCl$_3$ [H(69)CCl$_3$] is located above the platinum coordination plane, mainly contacting with the C(28)–C(29) alkynyl unit [H(69)–C(28),C(29) 2.491, 2.732 Å]. All these contacts are far shorter than the sum of the H and C van der Waals radii (1.2 and 1.70 Å, respectively).[59] The Pt ··· H separations to both HCCl$_3$ molecules [Pt(1) ··· H(69),H(70) 3.195, 3.236 Å] are clearly longer than the sum of the van der Waals radii (r_{Pt} = 1.7 Å, r_H = 1.2 Å), lying out of the usual range of Pt ··· H(–X) (X = C, N, O) contacts reported in the literature.[36,60,61] The most remarkable feature in the structure of the *para*-pyridylethynyl complex **9b**, is that, in spite of the presence of free alkyne, one of the molecules of water found in the crystal [H$_2$O(1)] acts as a donor towards two pyridine nitrogen atoms [N(1) and N(2)] of different molecular anions [Pt(C≡CC$_5$H$_4$N-4)$_4$]$^{2-}$ giving an extended one-dimensional chain, through moderate[62] O–H ··· N(py) interactions. The hydrogen atoms of this H$_2$O molecule were located from difference maps and refined isotropically [O(1)–H(70) 0.81(10) Å, O(1)–H(71) 0.72(6) Å]. The H ··· N [H(70)–N(1) 2.074 Å, H(71)–N(2) 2.173 Å] and O ··· N [O(1)–N(1) 2.855 Å, O(1)–N(2) 2.883 Å] interatomic distances, as well as the O–H ··· N angles [O(1)–H(70)–N(1) 162.47°, O(1)–H(71)–N(2) 169.52°], are similar to those described in other systems with this type of interaction.[62–66]

The remaining structural details are unexceptional. Thus, the complex anion of **6** has crystallographic inversion symmetry, with the Pt atom on a inversion center, which implies a precise planar coordination symmetry, whereas the complex anions of **4** and **9b** have also almost linear *trans* C–Pt–C linkages [175.7(4)–179.1(2)°]. The Pt–C$_\alpha$ [1.952(10)–2.047(10) Å] and C$_\alpha$≡C$_\beta$ bond lengths [1.146(13)–1.257(13) Å] are fairly typical of platinum–acetylide σ-bonding, and the ethynyl groups show the expected lineal arrangement [Pt–C≡C 172.4(9)–177.9(2)°; C≡C–C 174.6(8)–179.4(9)°]. What is perhaps more remarkable in the three molecular anions, is the different orientation of the aryl rings with respect to the platinum coordination plane. In **4**, and probably related to the presence of CHCl$_3$ molecules, the trifluoromethylphenyl rings are the less tilted out of the platinum coordination plane (4.00, 4.45, 19.87, 33.89°). In contrast to this, in **6** two of the *para*-cyanophenyl rings are inclined substantially (25.06, 63.12°) towards the platinum coordination plane, and in **9b** three of the pyridinic rings remain practically

perpendicular to this coordination plane (4.80, 67.06, 74.78, 78.91°), limiting the π-conjugation of two mutually *trans* ligands through the platinum center.

Optical and electrochemical properties

The electronic absorption of all new homoleptic tetraalkynyl platinate(II) compounds were registered in CH$_2$Cl$_2$ and, in order to check the influence of the solvent, the spectra of some selected complexes were also collected in acetone, toluene and acetonitrile (Table 3). The spectra (CH$_2$Cl$_2$) are dominated by two (**3, 4, 7, 8, 9b**), three (**1, 2, 5a, 6**) or even four (**5b, 9a**) intense absorption bands, which are particularly prominent in the case of complexes **7** and **8** containing ethynyl fragments as substituents. The high energy features are clearly due to π ⟶ π* transitions of the alkynyl ligands. The introduction of the Pt atom seems to affect the low energy bands, which are red-shifted to longer wavelengths, and have higher molar absorption coefficients compared to those of the free alkynes, indicating an enhancement in the degree of π-delocalization through the Pt atom. On the basis of previous assignments, and theoretical studies on neutral bis-alkynyl platinum complexes,[13,16,67–69] the low energy absorptions could be tentatively attributed to an admixture of π ⟶ π*(C≡CR) IL/d$_\pi$(Pt) ⟶ π*(C≡CR) MLCT. The involvement of the π*-C≡CR in the LUMO of these complexes is supported by the dependence of the low energy absorption on the nature of the alkynyl ligands. It is found that the low energy band shifts to lower energy according the following sequence: C≡C(4-OMe)C$_6$H$_4$ **5a** (344 nm) ~ C≡C(4-CH$_3$)C$_6$H$_4$ **2** (345 nm) > C≡C(3-OMe)C$_6$H$_4$ **5b** (347 nm) ~ C≡CPh **1** (347 nm) > C≡C(4-CF$_3$)C$_6$H$_4$ **4** (350 nm) > C≡C(4-Ph)C$_6$H$_4$ **3** (370 nm) > C≡C(4-C≡CPh)C$_6$H$_4$ **8** (374 nm) > C≡C(4-C≡CH)C$_6$H$_4$ **7** (376 nm) > C≡C(4-CN)C$_6$H$_4$ **6** (381 nm) > C≡CC$_5$H$_4$N-4 **9b** (398 nm) > C≡CC$_5$H$_4$N-2 **9a** (400 nm). This tendency is in agreement with the fact that electron-withdrawing substituents, or those which allow an increase in the degree of π-conjugation, tend to stabilize the π*-alkynyl based LUMO to yield red-shifted absorptions. The proposed assignment is additionally supported by DFT calculations (Gaussian 98 at the B3LYP level) on the ion [Pt{C≡C-(4-CN)C$_6$H$_4$}$_4$]$^{2-}$ of complex **6**, which reproduce its experimental structure well in solid state. The contour plots of the HOMO and LUMO are shown in Fig. 3. The relative

Table 4 Photophysical data for complexes **1**–**9** in KBr and in 10^{-3} M CH$_2$Cl$_2$ solutions

Compound	(T/K)	λ_{exc}/nm	λ_{em}/nm	ϕ	τ/μs
1	KBr (298)	362, 392, 423	447, 465, 484		1.73
	CH$_2$Cl$_2$ (298)	401, 443 (sh)	454, 493	0.0278[a]	
	CH$_2$Cl$_2$ (77)	289, 339, 357	447, 468, 493		
2	KBr (298)	366, 384, 447	456, 480, 502, 530		1.95
	CH$_2$Cl$_2$ (298)	403	413 (sh), 431 (sh), 457, 486 (sh)	0.0061[a]	
	CH$_2$Cl$_2$ (77)	281, 331, 341, 357 (sh)	447, 465, 475, 488		
3	KBr (298)	see Fig. S3	538, 580		
	CH$_2$Cl$_2$ (298)	443	525	0.0120[b]	
	CH$_2$Cl$_2$ (77)	391	519, 555		
4	KBr (298)	388, 413, 449	472		0.55, 1.74
	CH$_2$Cl$_2$ (298)	402	470	0.0045[a]	
	CH$_2$Cl$_2$ (77)	303, 351, 371	463, 483, 497, 512		
5a	KBr (298)	356, 390, 405, 437	446, 463, 486 (sh)		0.93, 4.58
	CH$_2$Cl$_2$ (298)	384	454	0.0084[a]	
	CH$_2$Cl$_2$ (77)	287, 334, 356	444, 468, 483, 494		
5b	KBr (298)	387, 399, 434	447, 512, 595 (sh)		
	CH$_2$Cl$_2$ (298)	404, 433 (sh)	458, 491 (sh)	0.0061[a]	
	CH$_2$Cl$_2$ (77)	286, 336, 356	451, 474, 484, 498		
6	KBr (298)	397, 421	502, 579[c]		7.93
	CH$_2$Cl$_2$ (298)	446, 465, 486	506, 528 (sh), 571 (sh)	0.0152[b]	
	CH$_2$Cl$_2$ (77)	337, 374, 397	498, 550, 584		
7	KBr (298)	443, 498 (sh)	599, 645 (sh)		
	CH$_2$Cl$_2$ (298)	424 (sh), 465, 497 (sh)	510, 517, 588 (sh)	0.0024[b]	
	CH$_2$Cl$_2$ (77)[d]	330, 350, 383	499, 528, 540, 553		
8	KBr (298)	548	608		
	CH$_2$Cl$_2$ (298)	466	513 (sh), 541 (max), 580 (sh)	0.0018[b]	
	CH$_2$Cl$_2$ (77)	390, 415	541, 570, 590, 608		
9a	KBr (298)	380	456, 505, 552		
	CH$_2$Cl$_2$ (298)	395, 405, 430	455, 488 (max), 576	0.0164[a]	
	CH$_2$Cl$_2$ (77)	345, 364	450, 468, 495		
9b	KBr (298)	397, 406, 428 (sh)	465, 488, 512, 540 (sh)		0.73, 0.26
	CH$_2$Cl$_2$ (298)	416	482	0.0451[b]	
	CH$_2$Cl$_2$ (77)	390	471, 496 (sh), 518 (sh)		

[a] measured using Coumarin 343 as a standard. [b] Measured using [Ru(bipy)$_3$]$^{2+}$ as a standard. [c] $\lambda_{exc} = 450$ nm (see text). [d] In 2×10^{-5} solution; in a 10^{-3} M solution the emission is dependent on the λ_{exc} used (see ESI,† Fig. S2).

HOMO   **LUMO**
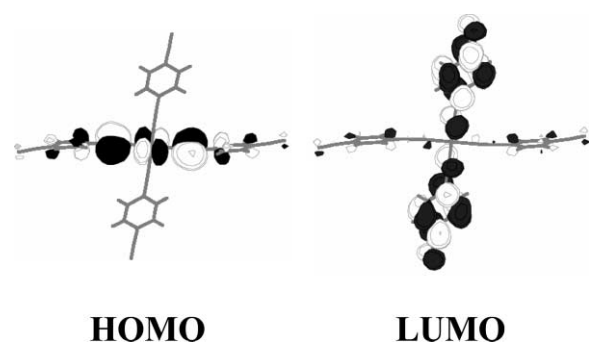
Fig. 3 Contour plots of the HOMO and LUMO of the anion [Pt{C≡C(4-CN)C$_6$H$_4$}$_4$]$^{2-}$ **6**.

composition of the different energy levels in terms of composing fragments are given in the ESI†(Table S1). As can be seen, the HOMO is a π orbital predominantly formed by two C≡C(4-CN)C$_6$H$_4$ mutually *trans* fragments, with additional contribution of Pt 5d (*ca*. 20%). The HOMO−1 and HOMO-2 have a similar composition,[70] the contribution of Pt being particularly notable in the HOMO−3 (56.4%). The LUMO (π*-C≡C–C$_6$H$_4$–CN in character) is mainly localized over the other two mutually *trans* alkynyl ligands, with a notable contribution of the (4-CN)C$_6$H$_4$ aromatic rings. The contribution of Pt in the LUMO and in the following unoccupied orbitals is negligible (see Table S1, ESI†), supporting some degree of MLCT to the optical transitions. The small solvatochromic shifts of the lowest energy absorption found in complexes **1**, **2**, **4** and **6** also suggest their charge-transfer nature. However, in complexes **4** (C≡C(4-CF$_3$)C$_6$H$_4$) and **6** (C≡C(4-CN)C$_6$H$_4$) a possible interaction between the *para*-substituents (–CF$_3$ and –CN) and the solvent is also likely.

The electrochemical behavior of our complexes were studied by cyclic voltammetry in CH$_2$Cl$_2$, and the results are also included in Table 3. In each case the cyclic voltammogram is characterized, within the solvent window, by a single irreversible oxidation wave in the range of 0.516 for **5a** to 0.916 for complex **9a**, which is attributed to the metal-centered oxidation from Pt(II) to Pt(III). This result is not unexpected in Pt(II) complexes; it is well documented that electrooxidation of Pt(II) complexes is often an irreversible process, because the electrogenerated radical cation readily undergoes rapid interaction with the solvent, leading to decomposition products. It has been also shown that, in some cases, oxidation of neutral platinum alkynyl complexes is followed by a rapid reductive elimination, as a means of returning electron density to the electron deficient metal fragment.[71] Although the tendency is less clear than that observed in the absorption spectra, in general, the oxidation is enhanced by electron donating substituents in *para*, such us OMe (**5a**) or *p*-Tol (**2**), while the presence of electron withdrawing groups, CF$_3$ (**4**) or CN (**6**), renders the platinum oxidation more difficult.

All complexes show emissive properties in solid state (R.T., KBr pellets) and in solution (fluid and glass). Some representative emission and excitation data obtained in solid state and in CH$_2$Cl$_2$ solution (r.t. and 77 K) are shown in Table 4, while corresponding data for selected complexes (**1**, **2**, **3** and **6**) in acetone, acetonitrile and toluene are given in the ESI†(Table S2).

The emission spectra in 77 K CH$_2$Cl$_2$ glass (10^{-3} M, 2×10^{-5} M for **7**) show structured bands with progressional spacing, suggestive of a combination of vibrational mode of C≡C and aryl moieties. The influence of the arylacetylide substituent is illustrated in Fig. 4. The extent of the observed shifts is greater than those seen in the absorption maxima and, with the exception of the pyridine derivative complexes (**9a**, $\lambda_{max} = 448$ nm. **9b**,
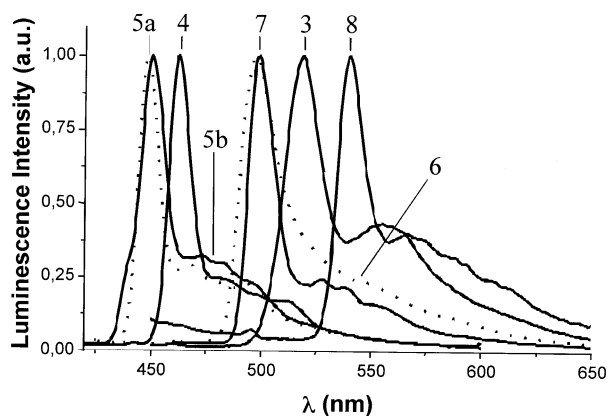
Fig. 4 Emission spectra of complexes **3–8** in CH$_2$Cl$_2$ at 77 K (concentration 10^{-3} M, 2 × 10^{-5} M for **7**).

Fig. 5 Excitation (λ_{em} = 550 nm) (—) and emission (λ_{exc} = 350 nm) (···) spectra of **6** in KBr pellets at room temperature and theoretical excitations (columns) obtained from the TD–DFT calculations.

λ_{max} = 471 nm.), the trends are similar. Complex **5a**, which bears the donor OMe group in *para* position, shows the highest emission energy (444 nm), while complex **8**, with the extended diynyl C≡C–C$_6$H$_4$–C≡C–Ph ligand, exhibits the lowest emission energy. The large Stokes shifts, lifetimes[72] and the observed trend is suggestive of an emission with predominantly IL character. Notwithstanding, a certain degree of a metal perturbed IL can not be discarded.[73] As can be seen in Table 4, the lowest quantum yields were found in complexes **7** (R = C≡C–C$_6$H$_4$–C≡C–H) and **8** (R = C≡C–C$_6$H$_4$–C≡C–Ph), containing the extended diynyl fragments. In agreement with the energy gap law,[74] in these complexes the smaller energy gap seems to increase the non-radiative decay rate. For complex **7**, using a concentration of 10^{-3} M, the emission (77 K) is dependent on the excitation energy (see Fig. S2 in ESI†). Thus, when the complex is excited at 360 nm, an asymmetric emission profile exhibiting a maximum at 506 nm with a long tail extending to 650 nm is observed. However, upon excitation at longer wavelengths (λ = 410 and 425 nm) two low energy emission maxima, at 523 and 580 nm, clearly increase from the tail, suggesting the presence of several emissive states.

In solution and in the solid state at r.t., the emission is less intense and the profiles are, in general, less structured, with their maxima slightly shifted (with exception of complex **8** in fluid solution, and complex **5b** in the solid state) to lower energies. In solid state, the emission profile of the biphenylethynyl derivative complex **3** is also dependent on the excitation energy (see Fig. S3 in ESI†) and for complexes **5b** and **6**, two emission bands were found at 447 and 512 nm and at 502 and *ca.* 579 nm, respectively; for complex **6**, the relative intensities of both bands are dependent on the excitation energy (see Fig. S4 in ESI†), suggesting again the presence of two closely lying emissive states of separate origins. For this complex (**6**) two different bands at 504 and 598 nm were also found in acetonitrile glass. The occurrence multiple luminescence is not unexpected, since it has been previously observed in other bis(alkynyl) platinum complexes.[30,32,73] For the anion complex of **6**, the main TD-DFT calculated excitation energies are illustrated in Fig. 5 (Table S3, ESI†), together with the experimental excitation spectrum observed by monitoring at λ = 550 nm, and the emission spectrum upon excitation at λ = 350 nm. The two intense calculated excitations at 399 and at 428 nm, which are in good agreement with the experimental excitations (397, 421 nm), are mainly attributed to HOMO−2 → LUMO+1 and HOMO−1 → LUMO (see Table S3, ESI†). As is shown in Table S1, the LUMO and LUMO+1 are essentially located on the arylacetylides (>98%), suggesting that the emission comes mainly from a triplet intraligand excited state of arylacetylides. This fact has also been previously observed in Au(I) and Ag(I) arylacetylides.[75,76]

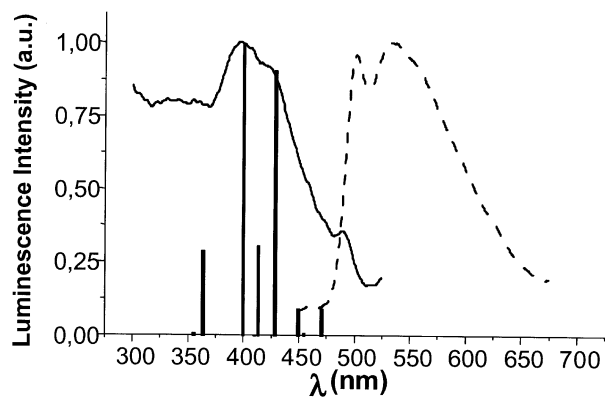It is interesting to note that the influence of the solvent is particularly notable in fluid solution for complex **1**. As can be seen in Fig. 6, the asymmetric emission with several shoulders, observed in CH$_2$Cl$_2$, in other solvents (λ_{max} = 454 nm) became well structured with maxima considerably shifted to higher energies (λ_{max} = 397 nm acetone, 396 nm acetonitrile, 399 nm toluene). This remarkable red shift (*ca.* 3100 cm^{-1}) observed in CH$_2$Cl$_2$ suggests the existence of some solvent–solute interaction with this solvent, that presumably stabilizes the emissive excited state.
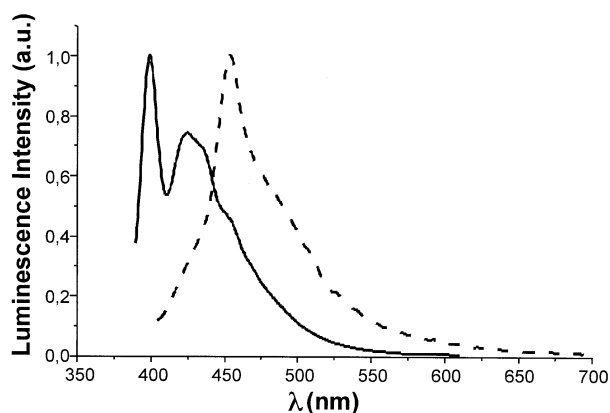

Fig. 6 Emission spectra of complex **1** in toluene (—) and CH$_2$Cl$_2$ (···) at room temperature (concentration 10^{-3} M).

Conclusions

In summary, a novel series of homoleptic aryl substituted (NBu$_4$)$_2$[Pt(C≡CC$_6$H$_4$X)$_4$] (**1–8**), where X is an electron-donating, -withdrawing, or -delocalizing substituent, and ethynylpyridine (NBu$_4$)$_2$[Pt(C≡CR)$_4$] (R = C$_5$H$_4$N-2 **9a**, C$_5$H$_4$N-4 **9b**) complexes have been synthesized and characterized, including X-ray diffraction for **3**, **6** and **9b**. Their photophysical and electrochemical properties have additionally been evaluated. Structured emissions attributed, on the basis of TD–DFT theoretical calculations on the anion [Pt{C≡C(4-CN)C$_6$H$_4$}$_4$]$^{2-}$ of complex **6**, to triplet intraligand excited states, which arise from an admixture of π → π*(C≡CR) IL and d$_\pi$(Pt) → π*(C≡CR) MLCT transitions, are observed in the emission spectra. The influence of the alkynyl substituent is illustrated in the tunability of the emission, which covers the range from 446 to 608 nm in the solid state. In some cases the emission profile is clearly the envelope of several closely bands, whose relative intensity is dependent on the excitation energy. Further investigation into the potential of these new anionic platinate complexes in the construction of heteropolynuclear platinum–M clusters is now in progress.

Experimental

General procedures

All reactions were performed under a nitrogen atmosphere using standard Schlenk techniques. Solvents were purified according to standard procedures. NMR spectra were recorded on a Bruker ARX-300 spectrometer. Chemical shifts are reported in ppm relative to external standards ($SiMe_4$ and $CFCl_3$) and all coupling constants are given in Hz. IR spectra were obtained on a Perkin-Elmer FT-IR Spectrum 1000 spectrometer, using nujol mulls between polyethylene sheets. Elemental analyses were carried out with a Perkin-Elmer 2400 CHNS/O or a Carlo Erba EA1110 CHNS-O microanalyzer. Mass spectra were recorded on a VG Autospec double-focusing mass spectrometer operating in the negative FAB mode (**2**) or a HP-5989B mass spectrometer using the ES($-$) technique (**3**–**9**). Cyclic voltammetric studies were performed using an EG&G-283 potenciostat/galvanostat. Anhidrous CH_2Cl_2 was used as the solvent under a nitrogen atmosphere, and 0.1 M tetra-(*n*-butyl)ammonium hexafluorophosphate was used as supporting electrolyte. Luminescence, as well as excitation spectra, were registered in a Perkin-Elmer Luminescence Spectrometer LS 50B with a red-sensitive photomultiplier type R928 and corrected for instrumental response. Emission lifetime measurements were performed in the frequency domain with a Fluorolog-3 model FL3-11 with Fl-1029 lifetime emission PMT assembly, using a 450 W Xe lamp. The solution emission quantum yields were measured by the Demas and Crosby method,[77] using $[Ru(bipy)_3]Cl_2$ in degassed water and Coumarin 343 in degassed ethanol as the standards. The complex $[PtCl_2(tht)_2]$[78] and the alkynes *para*-ethynylphenylbenzene,[79] *para*-ethynyl-cyanobenzene,[79] *para*-bis(ethynyl)benzene,[79] *para*-ethynyl-(phenylethynyl)benzene[80] and *para*-ethynylpyridine[81] were prepared by literature methods. Phenylacetylene, *para*-ethynyl-toluene, *para*-ethynyl(trifluromethyl)benzene, *para*-ethynyl-methoxybenzene, *meta*-ethynylmethoxybenzene, *ortho*-ethynyl-pyridine and ^nBuLi were used as received.

Computational details

The experimental crystal structure of the anion $[Pt\{C{\equiv}C-(4-CN)C_6H_4\}_4]^{2-}$ of complex **6** was used as model for the theoretical calculations. The density functional calculations were performed on isolated molecules using the Gaussian 98 program package[82] at the B3LYP level.[83] The basis set for the platinum atom was LANL2DZ,[84–86] with the corresponding ECP, and 6-31G(d,p) for the C, N and H atoms. The excitation energies, singlets and triplets, for $[Pt\{C{\equiv}C(4-CN)C_6H_4\}_4]^{2-}$ were obtained using the Time Dependent Theory (TD-DFT).

Synthesis

The complexes were prepared according to the two following general procedures given for complexes **2** and **3**. The synthetic and characterisation details of the remaining complexes (including ^{13}C NMR data for complex **1**) are given in the ESI. †

$(NBu_4)_2[Pt\{C{\equiv}C(4-CH_3)C_6H_4\}_4]$ 2. To a fresh (-20 °C) solution of $LiC{\equiv}C(4-CH_3)C_6H_4$ (9.65 mmol) in Et_2O (40 cm³), $[PtCl_2(tht)_2]$ (0.50 g, 1.13 mmol) was added. The mixture was stirred at this temperature for 5 min, and then was allowed to reach room temperature (*ca.* 20 min). The resulting white suspension was evaporated to dryness, and the final oily residue, which contains $Li_2[Pt\{C{\equiv}C(4-CH_3)C_6H_4\}_4]$, was treated with deoxygenated water (~40 cm³). The yellow aqueous solution was rapidly filtered under N_2 through Celite, and the filtrate treated with a solution of $(NBu_4)Br$ (0.91 g, 2.82 mmol) in 10 cm³ of H_2O, with vigorous stirring, yielding $(NBu_4)_2[Pt\{C{\equiv}C-(4-CH_3)C_6H_4\}_4]$ **2** as a pale yellow solid, which was filtered and washed with H_2O and air dried. (0.97 g, 76%) (Found: C, 71.70; H, 8.47; N, 2.78%. $C_{68}H_{100}N_2Pt$ requires C, 71.60; H, 8.84; N,

2.46%); $\tilde{v}_{max}/cm^{-1}$ (C≡C) 2081s; δ_H ($CDCl_3$, 293 K) 7.11 (8H, d, J(H–H) 6.2, CH, Tol), 6.87 (8H, d, J(H–H) 6.2, CH, Tol), 3.73 (16H, m, NCH_2–, NBu_4), 2.18 (12H, s, CH_3, Tol), 1.83 (16H, m, $-CH_2$–, NBu_4), 1.52 (m, 16H, $-CH_2$–, NBu_4) and 0.89 (24H, t, $-CH_3$, NBu_4); $\delta_C\{^1H\}$ (CD_3COCD_3, 223 K) 131.2 (s), 130.4 (s, CH), 128.9 (s), 128.0 (s, CH, Tol), 118.4 {s, ^1J(Pt–C) 989.2, C_a}, 102.1 {s, ^2J(Pt–C) 290.2, C_β}, 58.4 (s, N–CH_2–, NBu_4), 23.9 (s, $-CH_2$–, NBu_4), 20.3 (s, CH_3, Tol), 19.5 (s, $-CH_2$–, NBu_4) and 13.6 (s, $-CH_3$, NBu_4); m/z 540 [Pt(C≡CTol)$_3^-$, 100%], 425 [Pt(C≡CTol)$_2^-$, 83%]; $\varLambda_M$(acetone): 217 Ω^{-1} cm² mol^{-1}.

$(NBu_4)_2[Pt\{C{\equiv}C(4-Ph)C_6H_4\}_4]$ 3. $[PtCl_2(tht)_2]$ (0.30 g, 0.67 mmol) was added to a fresh (-40 °C) solution of $LiC{\equiv}C-(4-Ph)C_6H_4$ (4.07 mmol) in Et_2O (40 cm³). The mixture was stirred at low temperature for 5 min, and then was allowed to reach room temperature (*ca.* 30 min). The solvent was removed in vacuum, and the residue extracted with cold *i*-PrOH (~20 cm³) and filtered through Celite. Treatment of the filtrate with $(NBu_4)Br$ (0.55 g, 1.70 mmol) caused the precipitation of **3** as a yellow solid (0.21 g, 22%) (Found: C, 75.81; H, 7.58; N, 2.04%. $C_{88}H_{108}N_2Pt$ requires C, 76.10; H, 7.84; N, 2.02%); $\tilde{v}_{max}/cm^{-1}$ (C≡C) 2082s; δ_H ($CDCl_3$, 293 K) 7.64 (8H, d), 7.44 (m), 7.36 (24H, m), 7.27 [4H, t, (4-Ph)C_6H_4], 3.75 (16H, m, N–CH_2–, NBu_4), 1.90 (16H, m, $-CH_2$–, NBu_4), 1.57 (16H, m, $-CH_2$–, NBu_4) and 0.95 (24H, t, $-CH_3$, NBu_4); $\delta_C\{^1H\}$ ($CDCl_3$, 223 K) 141.1 (s), 135.2 (s), 132.0 (s, CH), 130.5 (s), 128.6 (s, CH), 126.44 (s, CH), 126.35 (s), 125.9 (s, CH, (4-Ph)C_6H_4), 117.4 {s, ^1J(Pt–C) 984.0, C_a}, 103.6 {s, ^2J(Pt–C) 285.0, C_β}, 58.9 (s, N–CH_2–, NBu_4), 24.3 (s, $-CH_2$–, NBu_4), 19.8 (s, $-CH_2$–, NBu_4) and 14.2 (s, $-CH_3$, NBu_4); m/z 1147 ([{Pt(C≡CC$_6$H$_4$Ph)}$_4$(NBu_4) + 1]$^-$, 6%), 726 [Pt(C≡CC$_6$H$_4$Ph)$_3^-$, 100%]; $\varLambda_M$(CH_3NO_2): 89 Ω^{-1} cm² mol^{-1}.

X-Ray crystallography study

Table 5 reports details of the structural analyses for all complexes. Yellow crystals of complexes **4** and **6** were obtained by slow diffusion of *n*-hexane into a chloroform (**4**) or a acetone (**6**) solution of each compound at -30 °C. For complex **4** two molecules of $CHCl_3$ and for complex **6** one molecule of water are found, respectively, in the asymmetric unit. In the case of complex **9b**, the aqueous filtrate obtained as described above in the Experimental section was left at room temperature overnight to yield yellow crystals that contain **9b**, as well as a molecule of *para*-ethynylpyridine and two molecules of water in the asymmetric unit. For all the complexes, X-ray intensity data were collected with a NONIUS kCCD area-detector diffractometer, using graphite-monochromated Mo-Kα radiation. Images were processed using the DENZO and SCALEPACK suite of programs,[87] carrying out the absorption correction for complex **6** at this point. For complexes **4** and **9b** the absorption correction was performed using SORTAV.[88] The structure of $6{\cdot}H_2O$ was solved by Patterson and Fourier methods using the DIRDIF92 program,[89] while the other two structures were solved by direct methods using the SHELXL-97 program.[90] The three structures were refined by full-matrix least squares on F^2 with SHELXL-97. All non-hydrogen atoms were assigned anisotropic displacement parameters. The hydrogen atoms H(70) and H(71), corresponding to one of the water molecules (H$_2$O(1)) of the structure of $9b{\cdot}HC{\equiv}CC_5H_4N-4{\cdot}2H_2O$ were located from difference maps and assigned isotropic parameters. The rest of the hydrogen atoms were constrained to idealized geometries fixing isotropic displacement parameters of 1.2 times the U_{iso} value of their attached carbon for the aromatic, the CH_2 and the $CHCl_3$ hydrogens and 1.5 for the methyl groups. Two residual peaks for **4** (2.06 and 1.93 e Å^{-3}) and one for **6** (1.09 e Å^{-3}) close to their respective Pt atoms were observed, but with no chemical significance. The low quality of the crystals of **6** does not allow the observation of reflection at low θ.

Table 5 Selected structural data for **4**·2CHCl₃, **6**·H₂O and **9b**·HC≡CC₅H₄N-4·2H₂O

	4·2CHCl₃	**6·H₂O**	**9b·HC≡CC5H4N-4·2H₂O**
Empirical formula	$C_{70}H_{90}Cl_6F_{12}N_2Pt$	$C_{68}H_{90}N_6OPt$	$C_{67}H_{97}N_7O_2Pt$
M_r	1595.23	1202.62	1227.60
T/K	123(1)	293(2)	173(1)
Crystal system	Monoclinic	Monoclinic	Monoclinic
Space group	$P2_1$	$P2_1/c$	$P2_1$
a/Å	12.1380(2)	10.9200(3)	13.5652(2)
b/Å	16.9520(3)	19.2720(5)	17.1763(2)
c/Å	18.0080(4)	15.7510(7)	14.2647(3)
α/°	90	90	90
β/°	95.7720(7)	91.7500(10)	105.2200(10)
γ/°	90	90	90
V/Å³	3686.60(12)	3313.26(19)	3207.10(10)
Z	2	2	2
D_c/g cm⁻³	1.437	1.203	1.269
μ/mm⁻¹	2.191	2.160	2.235
$F(000)$	1624	1248	1280
θ Range for data collection/°	3.41–27.48	4.09–24.71	1.90–27.88
Crystal size/mm	$0.60 \times 0.60 \times 0.40$	$0.40 \times 0.40 \times 0.40$	$0.20 \times 0.17 \times 0.12$
Data/restraints/parameters	16039/1/829	5614/0/353	14115/1/710
Goodness-of-fit on F^2	1.058	1.195	1.031
Final R indices [$I > 2\sigma(I)$]	$R_1 = 0.0403$, $wR_2 = 0.0925$	$R_1 = 0.0729$, $wR_2 = 0.1241$	$R_1 = 0.0414$, $wR_2 = 0.0774$
R indices (all data)	$R_1 = 0.0464$, $wR_2 = 0.0954$	$R_1 = 0.1454$, $wR_2 = 0.1518$	$R1 = 0.0565$, $wR_2 = 0.0830$
Max./min. el. dens/e Å⁻³	2.062/−1.443	1.094/−0.609	0.684/−1.565

References

1 J. Manna, K. D. John and M. D. Hopkins, *Adv. Organomet. Chem.*, 1995, **38**, 79.
2 J. Forniés and E. Lalinde, *J. Chem. Soc., Dalton Trans.*, 1996, 2587.
3 U. Belluco, R. Bertani, P. A. Michelin and M. Mozzon, *J. Organomet. Chem.*, 2000, **600**, 37.
4 H. Lang, D. S. A. George and G. Rheinwald, *Coord. Chem. Rev.*, 2000, **206–207**, 101.
5 K. Osakada and T. Yamamoto, *Coord. Chem. Rev.*, 2000, **198**, 379.
6 I. R. Whittal, A. M. McDonagh, M. G. Humphrey and M. Samok, *Adv. Organomet. Chem.*, 1998, **42**, 291.
7 Y. Lin, S. Jiang, K. Glusac, D. H. Powell, D. F. Anderson and K. S. Schanze, *J. Am. Chem. Soc.*, 2002, **124**, 12412.
8 N. J. Long, A. J. P. White, D. J. Williams and M. Younus, *J. Organomet. Chem.*, 2002, **649**, 94.
9 K. Hayashi, K. Onitsuka, N. Kobayashi and S. Takahashi, *Angew. Chem., Int. Ed.*, 2001, **40**, 4092.
10 P. Siemsen, U. Gubler, C. Bosshard, P. Günter and F. Diederich, *Chem. Eur. J.*, 2001, **7**, 1333.
11 M. S. Khan, M. R. A. Al-Mandhary, M. K. Al-Suti, A. K. Hisahm, P. R. Raithby, B. Ahrens, M. F. Mahon, L. Male, E. A. Marseglia, E. Tedesco, R. H. Friend, A. Köhler, N. Feeder and S. J. Teat, *J. Chem. Soc., Dalton Trans.*, 2002, 1358, and references therein.
12 K. Onitsuka, H. Kitajima, M. Fujimoto, A. Inchi, F. Takei and S. Takahashi, *Chem. Commun.*, 2002, 2576.
13 V. W. W. Yam, C. H. Tao, L. Zhang, K. M. C. Wong and K. K. Cheung, *Organometallics*, 2001, **20**, 453.
14 S. Leninger and P. J. Stang, *Organometallics*, 1998, **17**, 3981.
15 R. Ziessel, M. Hissler, A. El-ghayoury and A. Harriman, *Coord. Chem. Rev.*, 1998, **178–180**, 1251.
16 M. I. Bruce, K. Costuas, J. F. Halet, B. C. Hall, P. J. Low, B. K. Nicholson, B. W. Skelton and A. J. White, *J. Chem. Soc., Dalton Trans.*, 2002, 383.
17 J. A. Whiteford, C. V. Lu and P. J. Stang, *J. Am. Chem. Soc.*, 1997, **119**, 2524.
18 S. M. AlQuasidi, K. J. Galat, M. Chai, D. G. Ray, P. L. Rinaldi, C. A. Tessier and W. J. Youngs, *J. Am. Chem. Soc.*, 1998, **120**, 12149.

19 E. Bosch and C. L. Barnes, *Organometallics*, 2000, **19**, 5522.
20 S. S. Sun, J. A. Anspach, A. J. Lees and P. Y. Zavalij, *Organometallics*, 2002, **21**, 685.
21 Q.-Z. Yang, L.-Z. Wu, Z.-X. Wu, L. P. Zhang and C. H. Tung, *Inorg. Chem.*, 2002, **41**, 5653.
22 W. Lu, B. X. Mi, M. C. W. Chan, Z. Hui, N. Zhu, S. T. Lee and C. M. Che, *Chem. Commun.*, 2002, 206.
23 V. W. W. Yam, R. P. L. Tang, K. M. C. Wong and K. K. Cheung, *Organometallics*, 2001, **20**, 4476.
24 C. E. Whittle, J. A. Weinstein, M. W. George and K. S. Schanze, *Inorg. Chem.*, 2001, **40**, 4053.
25 V. W. W. Yam, K. M. C. Wong and N. Zhu, *J. Am. Chem. Soc.*, 2002, **124**, 6506.
26 J. V. Slageren, A. Klein and S. Zalis, *Coord. Chem. Rev.*, 2002, **230**, 193.
27 K. M. C. Wong, C. K. Hui, K.-L. Yu and V. W. W. Yam, *Coord. Chem. Rev.*, 2002, **229**, 123.
28 V. W. W. Yam, *Acc. Chem. Res.*, 2002, **35**, 555.
29 V. W. W. Yam, K. K. W. Lo and K. M. C. Wong, *J. Organomet. Chem.*, 1999, **578**, 3.
30 V. W. W. Yam, C. K. Hui, K. M. C. Wong, N. Zhu and K. K. Cheung, *Organometallics*, 2002, **21**, 4326.
31 J. P. H. Chartman, J. Forniés, J. Gómez, E. Lalinde, R. Merino and M. T. Moreno, *Organometallics*, 1999, **18**, 3353.
32 J. Forniés, J. Gómez, E. Lalinde and M. T. Moreno, *Inorg. Chim. Acta*, 2003, **347**, 145.
33 I. Ara, J. Forniés, J. Gómez, E. Lalinde, R. Merino and M. T. Moreno, *Inorg. Chem. Commun.*, 1999, **2**, 62.
34 I. Ara, J. Forniés, J. Gómez, E. Lalinde and M. T. Moreno, *Organometallics*, 2000, **19**, 3133.
35 I. Ara, J. R. Berenguer, J. Forniés, J. Gómez, E. Lalinde, A. Martín and R. Merino, *Inorg. Chem.*, 1997, **36**, 6461.
36 J. R. Berenguer, J. Forniés, J. Gómez, E. Lalinde and M. T. Moreno, *Organometallics*, 2001, **20**, 4847.
37 J. P. H. Charmant, J. Forniés, J. Gómez, E. Lalinde, R. I. Merino, M. T. Moreno and A. G. Orpen, *Organometallics*, 2003, **22**, 652.
38 J. P. H. Chartman, L. R. Falvello, J. Forniés, J. Gómez, E. Lalinde, M. T. Moreno, A. G. Orpen and A. Rueda, *Chem. Commun.*, 1999, 2045.
39 J. Forniés, J. Gómez, E. Lalinde and M. T. Moreno, *Inorg. Chem.*, 2001, **40**, 5415.
40 R. Nast and W. D. Heinz, *Chem. Ber.*, 1962, **95**, 1478.
41 C. Barral, R. Jiménez, E. Royen, V. Moreno and A. Santos, *Inorg. Chim. Acta*, 1978, **31**, 165.
42 R. Nast, J. Voss and R. Kramolowsky, *Chem. Ber.*, 1975, **108**, 1511.
43 A. Sebald, B. Wrackmeyer, C. R. Theocharis and W. Jones, *J. Chem. Soc., Dalton Trans.*, 1984, 747.
44 V. Zhon, A. M. Arif and J. S. Miller, *Chem. Commun.*, 1996, 1881.
45 P. Espinet, J. Forniés, E. Lalinde, F. Martínez, M. T. Moreno, A. Ruiz, M. Tomás and A. J. Welch, *J. Chem. Soc., Dalton Trans.*, 1990, 791.

46 P. Espinet, J. Forniés, M. Sotés, E. Lalinde, M. T. Moreno, A. Ruiz and A. J. Welch, *J. Organomet. Chem.*, 1991, **403**, 253.
47 J. Forniés, M. A. Gómez-Saso, E. Lalinde, F. Martínez and M. T. Moreno, *Organometallics*, 1992, **11**, 2876.
48 J. Forniés, E. Lalinde, A. Martín and M. T. Moreno, *J. Chem. Soc., Dalton Trans.*, 1994, 135.
49 I. Ara, J. R. Berenguer, J. Forniés, E. Lalinde and M. T. Moreno, *Organometallics*, 1996, **15**, 1820.
50 D. Zhang, D. B. McConville, C. A. Tessier and W. J. Youngs, *Organometallics*, 1997, **16**, 824.
51 J. R. Berenguer, J. Forniés, E. Lalinde and F. Martínez, *Organometallics*, 1996, **15**, 4537.
52 L. R. Falvello, J. Forniés, J. Gómez, E. Lalinde, A. Martín, M. T. Moreno and J. Sacristán, *Chem. Eur. J.*, 1999, **5**, 474.
53 H. C. Weiss, R. Boese, H. L. Smith and M. M. Haley, *Chem. Commun.*, 1997, 2403, and references therein.
54 M. F. Fan, Z. Lin, J. E. McGrady and D. M. P. Mingos, *J. Chem. Soc., Perkin Trans. 2*, 1996, 563.
55 T. E. Müller, D. M. P. Mingos and D. J. Williams, *J. Chem. Soc., Chem. Commun.*, 1994, 1787.
56 T. E. Müller, W. K. Choi, D. M. P. Mingos, D. Murphy, D. J. Williams and V. W. W. Yam, *J. Organomet. Chem.*, 1994, **484**, 209.
57 M. J. Alder, R. K. Flower and R. G. Pritchard, *J. Organomet. Chem.*, 2001, **629**, 153.
58 T. Steiner and M. Tamm, *J. Organomet. Chem.*, 1998, **570**, 235, and references therein.
59 A. Bonchi, *J. Phys. Chem.*, 1964, **68**, 441.
60 T. W. Hambley, *Inorg. Chem.*, 1998, **37**, 3767.
61 A. Martín, *J. Chem. Educ.*, 1999, **76**, 578.
62 B. Du, E. A. Meyers and S. G. Shore, *Inorg. Chem.*, 2000, **39**, 4639, and references therein.
63 E.-Q. Gao, L.-H. Yin, J.-K. Tang, P. Cheng, D.-Z. Liao, Z.-H. Jiang and S.-P. Yan, *Polyhedron*, 2001, **20**, 669.
64 N. Moliner, M. C. Muñoz and J. A. Real, *Inorg. Chem. Commun.*, 1999, **2**, 25.
65 C. T. Brewer, G. Brewer, M. Shang, R. Scheidt and I. Muller, *Inorg. Chim. Acta*, 1998, **278**, 197.
66 J. Lu, T. Paliwala, S. C. Lim, C. Yu, T. Niu and A. J. Jacobson, *Inorg. Chem.*, 1997, **36**, 923.
67 I. Ara, J. R. Berenguer, E. Eguizábal, J. Forniés, J. Gómez, E. Lalinde and J. M. Saez-Rocher, *Organometallics*, 2000, **19**, 4385, and references therein.
68 N. J. Long, A. J. Martin, R. Vilar, A. J. P. White, D. J. Williams and M. Younus, *Organometallics*, 1999, **18**, 461.
69 M. S. Khan, A. K. Kakar, S. L. Ingham, P. R. Raithby, J. Lewis, B. Spencer, F. Wittmann and R. H. Friend, *J. Organomet. Chem.*, 1994, **472**, 247.
70 The composition of HOMO−1 is mainly based on the other two mutually *trans* alkynyl fragments, while the HOMO−2 is building up from the four alkynyl fragments.
71 M. Sato, E. Mogi and S. Kumakura, *Organometallics*, 1995, **14**, 3157.
72 Due to instrumentation limitation, lifetimes were measured only in solid state, and for some complexes the intensity of the luminescence was too low to obtain reliable values.
73 V. W. W. Yam, K.-L. Yu, K. M. C. Wong and K. K. Cheung, *Organometallics*, 2001, **20**, 721.
74 J. S. Wilson, N. Chawdhury, M. R. A. Al-Mandhary, M. Younus, M. S. Khan, P. R. Raithby, A. Köhler and R. H. Friend, *J. Am. Chem. Soc.*, 2001, **123**, 9412.
75 H. Y. Chao, W. Lu, Y. Li, M. C. W. Chan, C. M. Che, K. K. Cheung and N. Zhu, *J. Am. Chem. Soc.*, 2002, **124**, 14696.
76 W. Lu, H. F. Xiang, N. Zhu and C. M. Che, *Organometallics*, 2002, **21**, 2343.
77 J. N. G. Demas and A. Crosby, *J. Phys. Chem.*, 1971, **75**, 991.
78 R. Usón, J. Forniés, F. Martínez and M. Tomás, *J. Chem. Soc., Dalton Trans.*, 1980, 888.
79 S. Takahashi, Y. Kuroyama, K. Sonogashira and N. Hagihara, *Synthesis*, 1980, 627.
80 O. Lavastre, S. Cabioch, P. H. Dixneuf and J. Vohlidal, *Tetrahedron*, 1997, **53**, 7595.
81 L. D. Ciana and A. Haim, *J. Heterocycl. Chem.*, 1984, **21**, 607.
82 M. J. Frisch, G. W. Trucks, H. B. Schlegel, G. E. Scuseria, M. A. Robb, J. R. Cheeseman, V. G. Zakrzewski, J. A. Montgomery, Jr., R. E. Stratmann, J. C. Burant, S. Dapprich, J. M. Millam, A. D. Daniels, K. N. Kudin, M. C. Strain, O. Farkas, J. Tomasi, V. Barone, M. Cossi, R. Cammi, B. Mennucci, C. Pomelli, C. Adamo, S. Clifford, J. Ochterski, G. A. Petersson, P. Y. Ayala, Q. Cui, K. Morokuma, P. Salvador, J. J. Dannenberg, D. K. Malick, A. D. Rabuck, K. Raghavachari, J. B. Foresman, J. Cioslowski, J. V. Ortiz, A. G. Baboul, B. B. Stefanov, G. Liu, A. Liashenko, P. Piskorz, I. Komaromi, R. Gomperts, R. L. Martin, D. J. Fox, T. Keith, M. A. Al-Laham, C. Y. Peng, A. Nanayakkara, M. Challacombe, P. M. W. Gill, B. G. Johnson, W. Chen, M. W. Wong, J. L. Andres, C. Gonzalez, M. Head-Gordon, E. S. Replogle and J. A. Pople, GAUSSIAN 98 (Revision A.11), Gaussian, Inc., Pittsburgh, PA, 2001.
83 C. Lee, W. Yang and R. G. Parr, *Phys. Rev. B*, 1988, **37**, 785.
84 P. J. Hay and W. R. Wadt, *J. Chem. Phys.*, 1985, **82**, 270.
85 W. R. Wadt and P. J. Hay, *J. Chem. Phys.*, 1985, **82**, 284.
86 P. J. Hay and W. R. Wadt, *J. Chem. Phys.*, 1985, **82**, 299.
87 Z. Otwinowski and W. Minor, *Methods Enzymol. A: Macromol. Crystallogr.*, 1997, **276**, 307.
88 R. H. Blessing, *Acta Crystallogr., Sect. A*, 1995, **51**, 33.
89 P. T. Beursken, G. Beursken, W. P. Bosman, R. de Gelser, S. García-Granda, R. O. Gould, J. M. M. Smith and C. Smykalla, The DIRDIF92 program system, Technical Report of the Crystallography Laboratory, 1992.
90 G. M. Sheldrick, SHELX-97, a program for the refinement of crystal structures, 1997.